On Modeling Spectral Dissipation due to Wave Breaking for Ocean Wind Waves

Michael L. Banner[1] and Russel P. Morison

Climate and Environmental Dynamics Laboratory, School of Mathematics,
The University of New South Wales, Sydney 2052, Australia

1. Introduction

Over the past decade, the overall turbulent kinetic energy (TKE) dissipation rate in the upper ocean has been measured, and these measurements have revealed greatly enhanced levels over conventional rough wall estimates (eg. Terray et al, 1996, Gemmrich and Farmer, 2004). This enhancement has been attributed primarily to wave breaking. Further, according to available knowledge, almost the *entire* wind input momentum and energy fluxes to the waves leave the wave field locally via wave breaking to drive currents and generate turbulence, respectively, in the upper ocean (Donelan, 1998). This suggests strongly that dissipation through wave breaking is a very significant process in the wind wave evolution process. Yet, it remains the least well-understood source term, in relation to the other two source terms – wind input and nonlinear spectral transfer.

Wave breaking in deep water is due to wave energy focusing (convergence), and often occurs at the envelope maxima of wave groups (Holthuijsen and Herbers, 1986). Breaking produces complex overturning of the sea surface, leading to enhanced interfacial fluxes (eg. Melville, 1994). The highly nonlinear nature of breaking in physical space presents substantial challenges for modeling this process in the customary phase-unresolved spectral domain used in contemporary wind wave evolution models.

Nevertheless, from the observational perspective described in the opening paragraph, it appears compelling to seek a plausible modeling framework for representing wave breaking influence at different spectral scales in modern sea state forecast models. This contribution first describes a particularly interesting field data set, and then how it allows a refinement of the source terms for wind input and dissipation that provides a self-consistent account of the observations. This is part of our ongoing effort to extend spectral modeling to provide more reliable and informative severe sea state forecasts that include breaking waves.

2. Observations and modeling objectives

2.1 *Available field observations*

The breaking wave data used in this study was reported in preliminary form by Gemmrich (2005). In brief, the FAIRS (Fluxes, Air-Sea Interaction and Remote Sensing) experiment took place in September-October 2000 from aboard the research platform FLIP, roughly 150 km off Monterey, California. Two downward looking monochrome video cameras mounted on the starboard boom recorded whitecap events. There were synchronous measurements of wind speed and direction, wind stress and wave height. Figure 1 summarizes the observed conditions and salient data. A unique feature of this data set is the measurements of wave breaking statistics for a developing wind sea (U_{10}/c_p~1.2), in addition to those for mature sea conditions. Such data for growing wind seas was not previously available.

Corresponding author email address: m.banner@unsw.edu.au
[1] also Lamont-Doherty Earth Laboratory, Columbia University, Palisades, NY

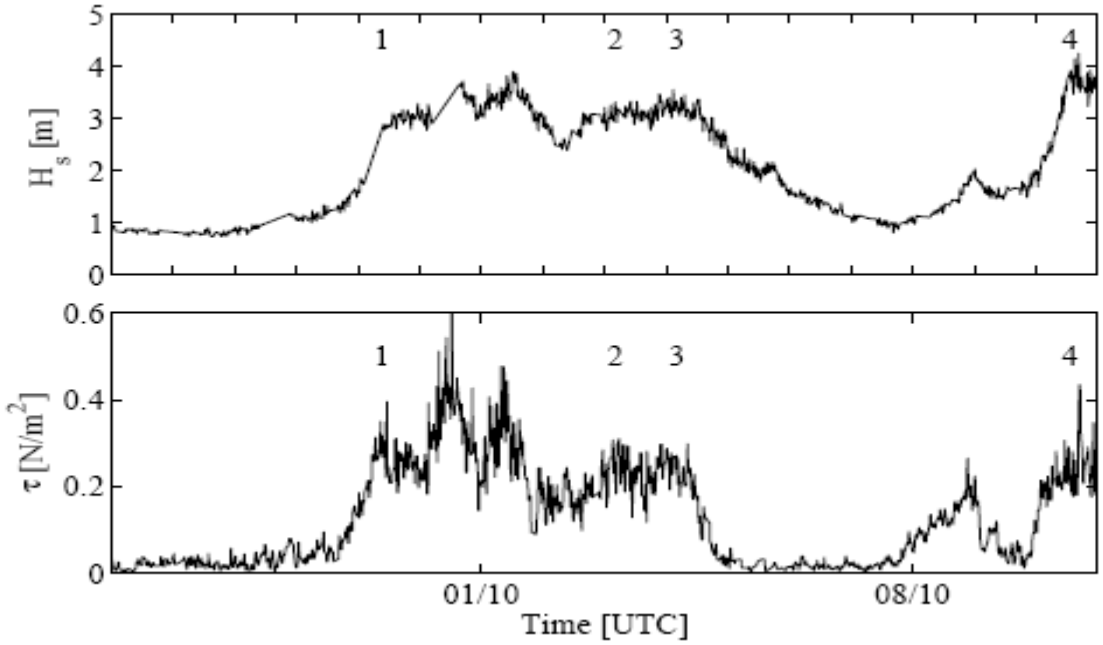

Figure 1. Significant wave height (H_s) and wind stress (τ) during the FAIRS experiment. The wind direction was around 300^o for most of the observational period. Periods 1 (growing seas) and 3 (mature seas) are of particular interest in this study, during which the mean wind was measured to be 12 m/s.

Figure 2 below summarizes the differences in the breaking probabilities between developing (U_{10}/c_p~1.2) and mature seas (U_{10}/c_p<0.9). The crucial feature evident for the developing seas is the significant breaking occurring at the *spectral peak* wave scales. Note that according to all variants of the wind input source term, there is relatively low wind input to the spectral peak waves for U_{10}/c_p~1.2, yet the observations confirm the presence of dominant wave breaking, as measured by the breaker speeds. This excludes the possibility that these are shorter waves breaking at the crests of the dominant waves.

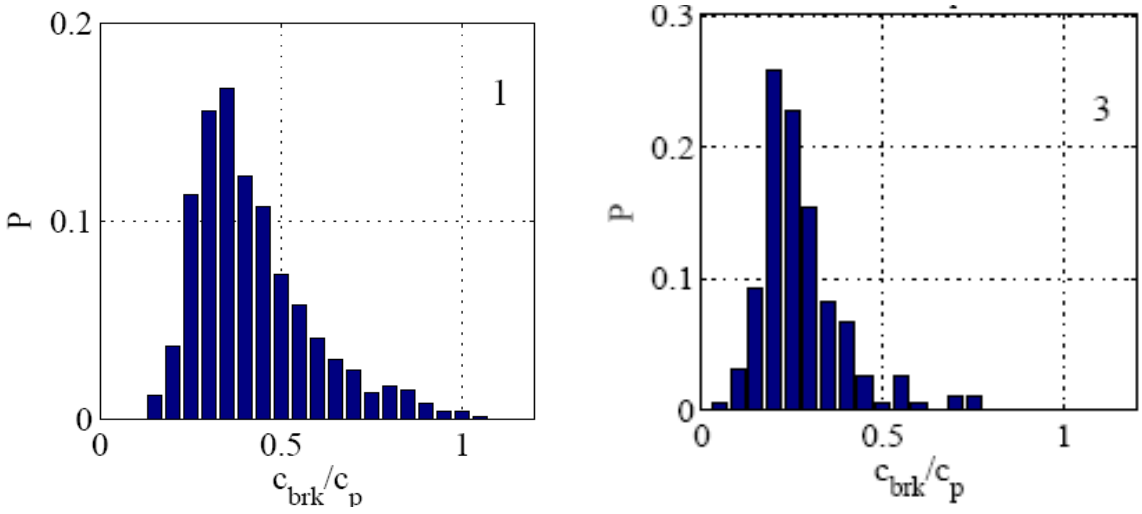

Figure 2. Probability distribution of breaking waves as a function of wave speed relative to the spectral peak, for period 1 (growing seas) and 3 (mature seas). Note that breaking events occur at the spectral peak ($0.8<c_{brk}/c_p<1.2$) for period 1, but not for period 3.

2.2 *Modeling objectives*

These observations add significantly to existing benchmarks for realistic research wind wave model predictions. These benchmarks now comprise:
I. evolution of mean wave energy and peak frequency
II. spectral tail properties: mean directional spreading with k/k_p; spectral saturation; level and exponent of 1D transect k-spectrum
III. a check on relative size of wave-induced stress level in computational domain
IV. prediction of breaking crest length/unit area spectral density at different wave ages.

Our present goal is to be able to reproduce the observed properties in I-IV above using numerical forecasts based on our wind wave model source terms, as described below.

3. Overview of wind wave modeling approach

3.1 *Radiative transfer equation*

The spectral evolution of the wave height spectrum was computed via the radiative transfer equation (deep water, no currents):

$$\frac{\partial F}{\partial t} + c_g \cdot \nabla F = S_{tot} \qquad (1)$$

where $F = F(k,\theta)$ is the directional wave spectrum, c_g is the group velocity. The total source term $S_{tot} = S_{in} + S_{nl} + S_{ds}$, where S_{in} is the atmospheric input spectral source term, S_{nl} is the nonlinear spectral transfer source term representing nonlinear wave-wave interactions and S_{ds} is the spectral dissipation rate, primarily due to wave breaking.

3.1.1 *Wind input source term S_{in}*

The magnitude and spectral composition of the wind input source term S_{in} remains imprecisely known, despite very considerable observational and theoretical study over the past few decades. In the context of developing a model framework for forecasting breaking properties, we investigated a number of proposed S_{in} formulations. The forms of S_{in} we implemented were (i) Hsiao-Shemdin (1983) and (ii) Janssen (1991). We note that (i) is based on a set of field observations using a wave-follower while (ii) is based on the critical layer theory of Miles (1957) and is tuned closely to available field measurements of Snyder *et al* (1981) and laboratory measurements (Plant, 1982). The differences between these are indicative of the level of uncertainty between nominal S_{in} forms used in different contemporary wave models. Figure 3 below compares their nondimensional growth rates β for developing and mature wind seas. Note that they differ considerably as regards their spectral levels for weakly and strongly forced scales.

We made a minor modification to the Janssen (1991) input source term that is in the spirit of the notion of sheltering (eg. Makin and Kudryavtsev, 2001), amongst others. This reduces the driving stress to the shorter waves due to reduction of part of the wave stress by the longer waves. It allowed us to fine tune the integrated wind input energy flux to balance the integrated energy loss rate due to breaking. This is an important validation check for the modeling, and we found that our sheltering algorithm provided wind stress estimates that agreed very closely with the observed levels as the wind sea aged. The nonlinear transfer term had zero net integral at all times. The modified input growth rate used in our calculation is also shown in Figure 3.

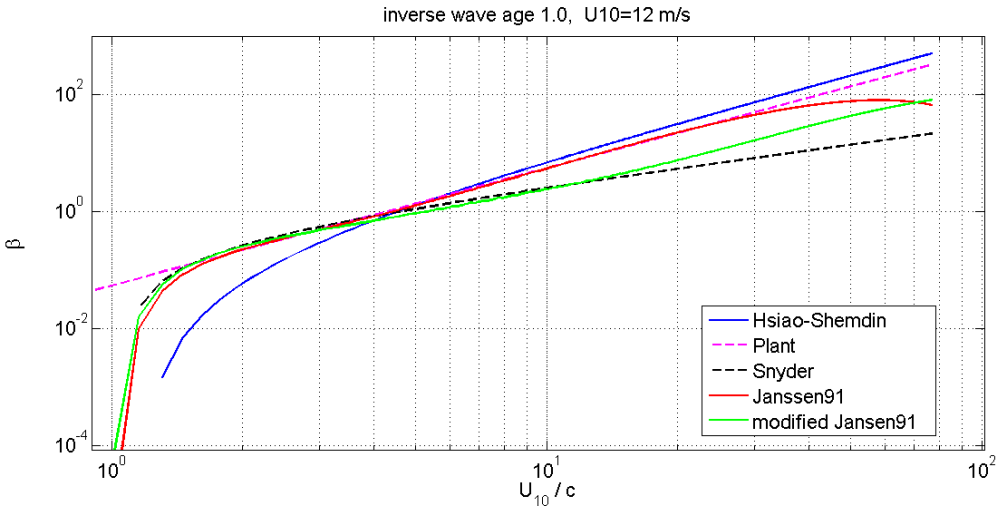

Figure 3. Plot showing the considerable differences between the spectral growth rate β of selected commonly implemented forms of S_{in} for maturing seas (U_{10}/c_p~1.0). The modified Janssen91 curve shows the extent of sheltering introduced for the slower moving, shorter wave components. This is sufficient to align the computed windstress with observed levels.

3.1.2 *Nonlinear spectral transfer source term S_{nl}*

We used the 'exact' form of S_{nl} to avoid the known errors associated with 'discrete interaction approximation' implementations in use operationally. The version used is a recent update (Don Resio, private communication) of Tracy and Resio (1982) that has directional coverage of ±180°.

3.1.3 *Spectral dissipation rate term S_{ds}*

We used a saturation based form of S_{ds} evolved from the form discussed by Alves and Banner (2003). This form was motivated by the observed threshold behavior reported by Banner *et al.* (2002) for the wave breaking probability in the spectrum. This was defined as the ratio of the passage rate past a fixed point of breaking crests with velocities in (*c*, *c*+*dc*) to the passage rate past a fixed point of all wave crests with velocities in (*c*, *c*+*dc*). The sea state threshold variable was the azimuth-integrated spectral saturation $\sigma(k) = k^4 \Phi(k) = (2\pi)^4 f^5 F(f)/2g^2$, normalized by the mean spectral spreading width $\bar{\theta}(k)$. Here $\Phi(k)$ and $F(f)$ are the spectra of wave height as a function of scalar wavenumber and frequency, respectively. The observed breaking probabilities for different centre frequencies relative to the spectral peak were then found to have a well-defined threshold behaviour, with a common breaking threshold value $\tilde{\sigma}_T \sim 0.0045$, as seen in Figure 4 below, reproduced from (Banner et al., 2002).

Based on the strongly thresholded behaviour indicated by these observations of breaking probability, we refined the $S_{ds}(\boldsymbol{k})$ term proposed by Alves and Banner (2003). This form embodies saturation threshold behaviour, based on treating waves in different directional spectral bands as nonlinear wave groups. It is in the spirit of the nonlinear forms of S_{ds} discussed thoughtfully by Donelan and Yuan in §II.4 of Komen et al. (1994).

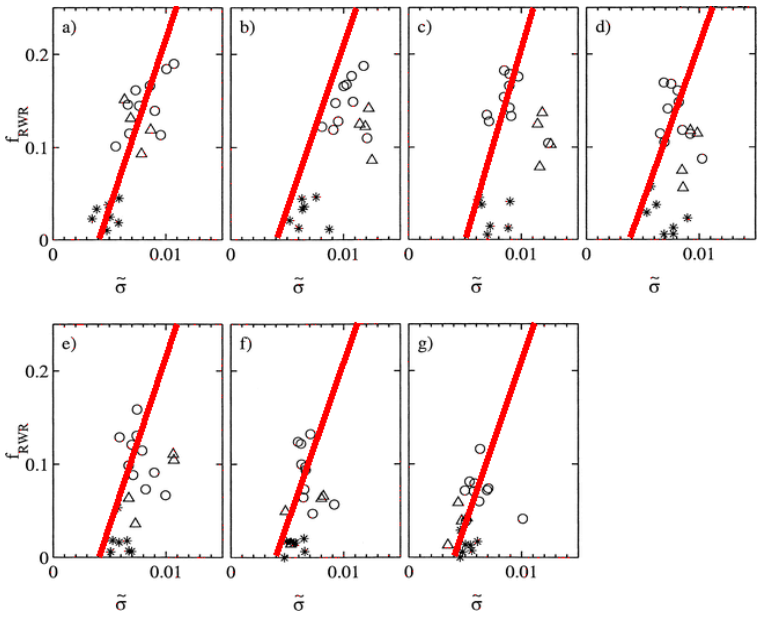

Figure 4. Breaking probability f_{RWR} against $\tilde{\sigma}$, the azimuth-integrated saturation normalized by the mean spectral spreading width $\bar{\theta}$ for the range of non-dimensional centre frequencies f_c/f_p investigated: (a) f_c/f_p = 1.0 (b) f_c/f_p = 1.16 (c) f_c/f_p = 1.35 (d) f_c/f_p = 1.57 (e) f_c/f_p = 1.83 (f) f_c/f_p = 2.13 (g) f_c/f_p = 2.48. Each data point is a one-hour data record from three North Pacific storms, as described in (Banner et al., 2002). Note the threshold behaviour and close correspondence between different spectral bands.

The form of S_{ds} used in this study is shown below. It uses a power law function of the normalized spectral saturation ratio to reflect the observed breaking threshold behaviour, and refines the form proposed by Alves and Banner (2003). The form used here is

$$S_{ds}(k,\theta) = C\,[(\tilde{\sigma} - \tilde{\sigma}_T)/\tilde{\sigma}_T)^a\,\tilde{\sigma}^b + \varepsilon_{res}]\,(\sigma/\sigma_m)^c\,\omega F(k,\theta) \qquad (2)$$

In (2) σ and $\tilde{\sigma}$ are the saturation and saturation normalized by the directional spreading width, $\tilde{\sigma}_T$ is threshold normalized saturation and σ_m is the saturation at k_m, the mean wavenumber at the transition from the peak enhancement region to the spectral tail. The breaking threshold switching exponent *a* was taken as 2, with *b* taken as 0 and *c* taken as 4, based on matching to the high wavenumber form of $S_{in}(k)$. The tuning constant *C* was chosen to provide the optimal match to observed duration evolution data of the spectral peak energy and peak frequency (eg. Young, 1999). ε_{res} is a small background residual dissipation coefficient that is consistent with observed decay rates of swell leaving storm areas.

This form of S_{ds} based on the (smoothed) local saturation ratio refines the integral wave steepness threshold used in the quasilinear form of S_{ds} presently used in most operational wave models.

3.3 *Extraction of breaking wave properties*

The observations provide measured spectral density of breaking crest length/unit area Λ against wave speed *c*, while the model output is $S_{ds}(k)$. The connection between the two is assumed to be given by the scalar form of equation (6.3) in Phillips (1985):

$$S_{ds}(c)\,dc = b\,g^{-1}c^5\Lambda(c)\,dc \qquad (3)$$

where the non-dimensional coefficient *b* reflects the breaking strength. Breaking of the dominant wind waves is known to attenuate short wave energy so the local scale association implicit in (3) is a potential over-simplification. Even in assuming (3), the dependence of *b* on wave variables is not yet understood. The expectation is that *b* should increase systematically with wave nonlinearity. In a recently submitted paper, Banner and Peirson (2006) found a strong correlation for *b* with the energy convergence rate within nonlinear wave groups. In the absence of more precise data at this time, a representative mean value of $b=2.5\times10^{-5}$ was assumed here, based on a detailed analysis of the FAIRS breaking measurements by Gemmrich (private communication) and described elsewhere in these proceedings.

3.4 *Full bandwidth computation of duration-limited wind wave evolution*

Computations of the directional wave spectrum were made for the full spectral bandwidth covering 0.02 Hz to 3.0 Hz, using the source terms described in §3.2 above. In this contribution we focus on the case of a steady forcing wind speed of U_{10} = 12 m/s, noting that during periods 1 and 3 annotated in Figure 1, the prevailing mean wind speed U_{10} ~12 m/s was blowing for 6-8 hours *prior* to the wave measurements reported here.

Of particular interest was benchmark IV, a comparison of forecast and observed breaking wave properties, especially at the spectral peak where the form (3) is most likely to be valid. This particular comparison has not been undertaken previously. Not only does this provide a tighter constraint on the form of the spectral dissipation rate source term, but it has the additional benefit of reducing the uncertainty in the form of S_{in}, as is explained below.

4. Results

4.1 *Preliminary validations*

We began by validating our model results for wave energy and spectral peak frequency against the duration-limited data trend curve given by Young (1999, §5.3.4) (benchmark I in §2.2). It is seen that our model closely reproduces these data trends.

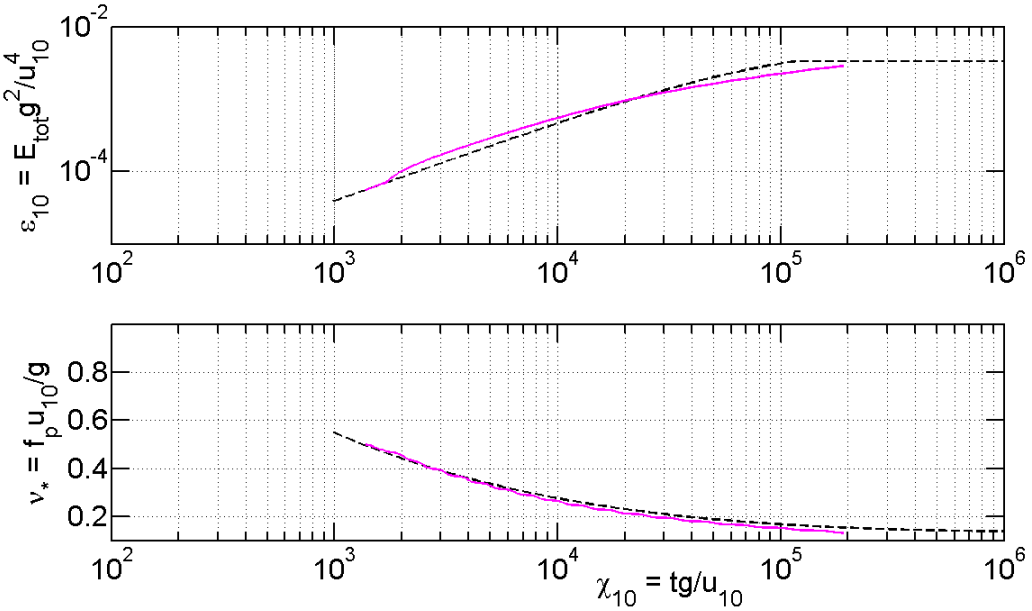

Figure 5. Evolution of nondimensional mean wave energy (upper panel) and spectral peak frequency (lower panel) against nondimensional time for duration limited growth. The background dashed lines are the trends of the data collated by Young (1999).

The results for the additional benchmarks II and III in §2.2 are shown in Figures 6 and 7. These spectral measures have been checked against available data and are in close accord with these data.

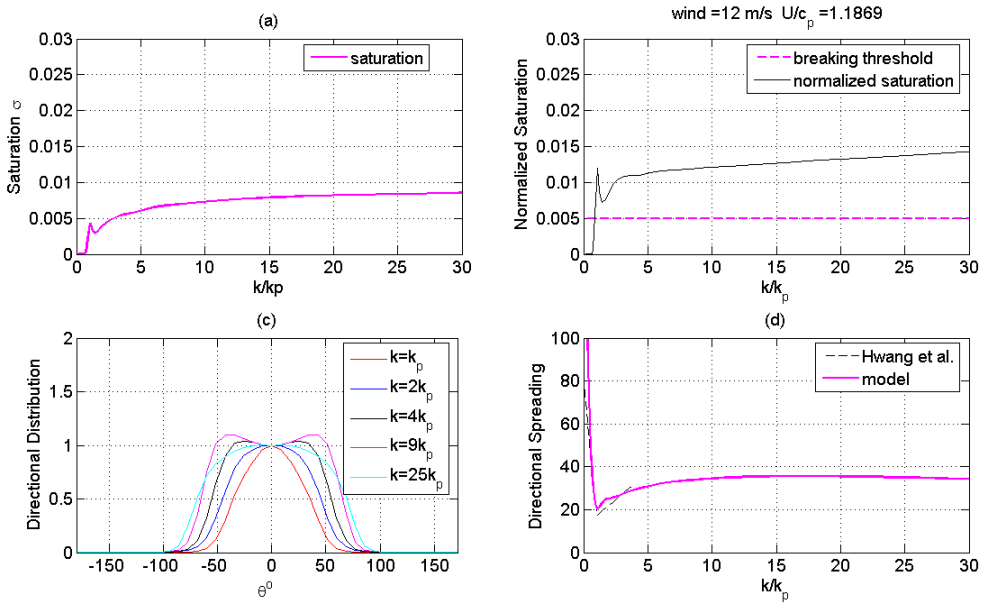

Figure 6. The upper two panels show the spectral saturation (the azimuth averaged fourth moment of the wavenumber spectrum). The left panel shows how the saturation changes with distance from the spectral peak. The right panel shows the corresponding behaviour of the saturation normalized by the corresponding mean directional spreading width. The directional spreading properties are seen in the lower two panels. The weakly bimodal angular spreading distributions at various distances from the spectral peak are seen in the left panel, while the right panel shows how the mean spreading width varies with distance from the spectral peak. The angle shown is the half-width in degrees. The data in (d) is from Hwang *et al*. (2000).

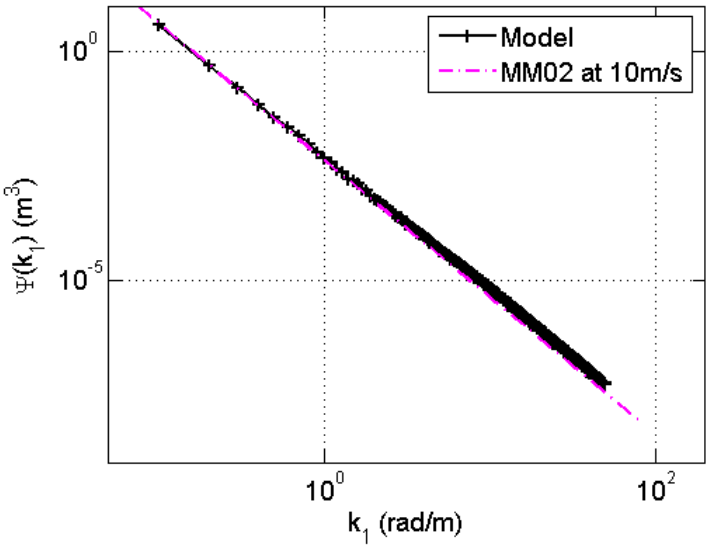

Figure 7. One-dimensional (k_1) transect spectrum in the upwind-downwind direction, showing a close correspondence with the measured k_1^{-3} data trend of Melville and Matusov (2002), measured for very old wind seas in the 8-13 m/s range.

The remaining benchmark III is concerned with the relative size of wave-induced stress level in computational domain. The sum of the wave stress and the viscous tangential stress equals the total wind stress, which was measured in the FAIRS experiment and is shown above in the lower panel of Figure 1.

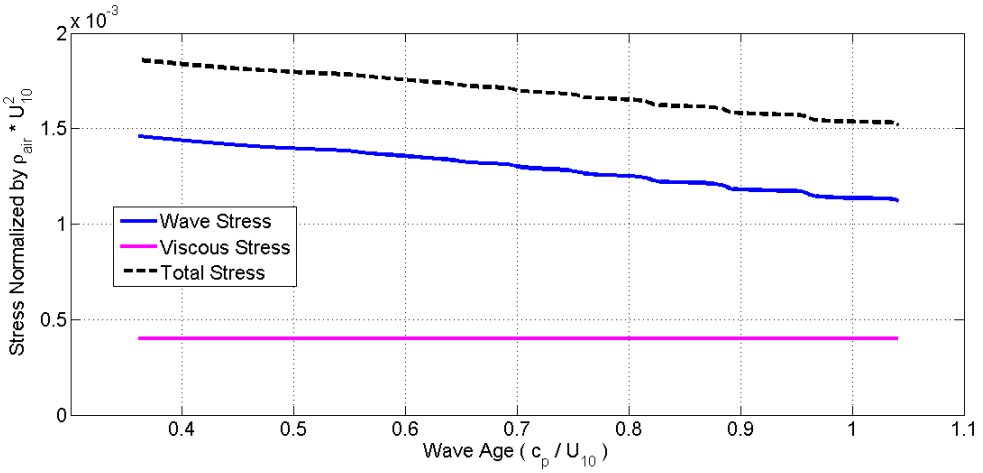

Figure 8. Behavior of the normalized wave stress and viscous tangential stress as the wind sea ages. The viscous stress follows the estimate by Banner and Peirson (1998).

The measured wind stress in Figure 1 is equivalent to a drag coefficient of 1.6×10^{-3} for developing seas during period 1 (wave age ~ 0.84) and 1.4×10^{-3} for the mature wind seas (wave age > 1.11) during period 3. The model results agree closely with these observed levels.

4.2 *Wave breaking forecasts*

This is the most challenging aspect of the model validation. The validation needs to reproduce the observed breaking statistics. Recent remotely sensed measurements of $\Lambda(c)$, the spectral density of breaking crest length per unit area of sea surface, travelling with speeds in the range (c, c+dc), provide a suitable observational database. The spectral peak region provides for the most straightforward initial comparison, and we will concentrate on this region in this paper. For slower moving shorter waves, it is very evident that the model results depart substantially from the observations, with the former increasing while the latter maximizes and then decreases towards slower wave speeds. The model behavior is constrained by equation (3), for which we can easily envisage the alternate possibility of a form with a nonlocal dependence. As an illustration, it is entirely consistent with observations that breaking longer waves attenuate short wave energy. This is additional to the short wave dissipation through their breaking. However, this will be left for a future paper, and we will focus on the spectral peak region where these issues do not arise.

Figures 9 and 10 show the modeled and observed spectral distributions of $\Lambda(c)$ for different wave ages. The behaviour at the spectral peaks of the developing seas (period 1 where c_{peak} = 10 m/s) and mature seas (period 3 where c_{peak}=12.5 m/s) are the focus of the comparison. The model predictions for the shorter waves are clearly not in accord with the data, as foreshadowed above, and will be the subject of a future paper. The results indicate very encouraging agreement between observed and forecast levels during both of

these observational periods. Further such comparisons with data are now needed to establish the robustness of the modeling approach used here.

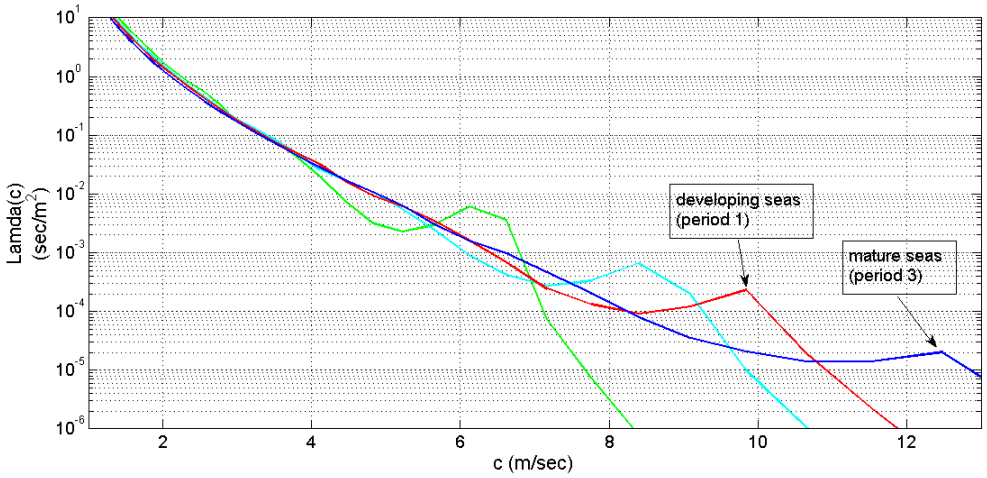

Figure 9. Model forecast of breaking wave crest length spectral density $\Lambda(c)$ at different wave ages during the evolution for U_{10}=12 m/sec. Of particular interest are the red and dark blue curves, corresponding to the sea state wave age conditions during periods 1 and 3, where the spectral peak speeds were 10 m/sec and 12.5 m/sec respectively. The green and cyan curves, for much younger seas, are included for interest.

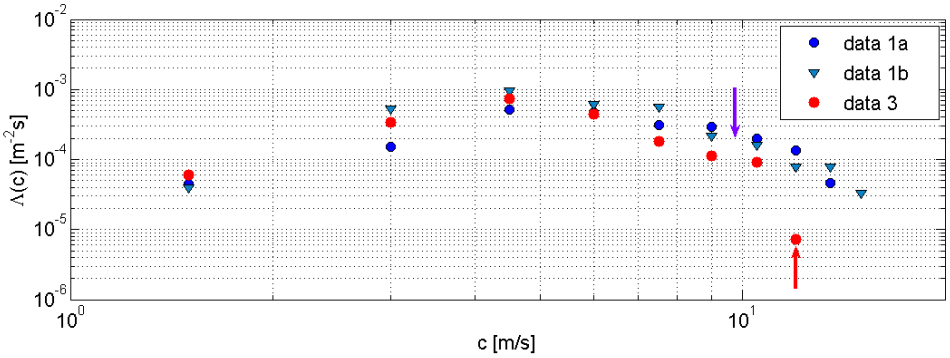

Figure 10. Measured breaking wave crest length spectral density $\Lambda(c)$ for period 1 (blue circles and triangles) and period 3 (red circles) during the evolution for U_{10}=12 m/sec. The red and blue arrows indicate the spectral peaks corresponding to the wave age conditions during periods 1 and 3, where the spectral peak speeds were 10 m/sec and 12.5 m/sec respectively.

A comparison of the observed and model results shows that the spectral peak level of Λ changes over an order of magnitude as the wave age c_p/U_{10} changes from 0.83 (period 1) to 0.96 (period 3). Underlying this transition is the source term balance, shown below in Figure 11. The interesting feature is that even though the wind input to the dominant waves decreases to well below the dissipation rate as the wave speed approaches the wind speed, the dominant wave saturation level (and steepness) remains sufficiently large for

the breaking to occur through nonlinear interactions (eg. wave group modulations), as reported in Banner and Peirson (2006). This is built into our proposed form (2) for S_{ds}.

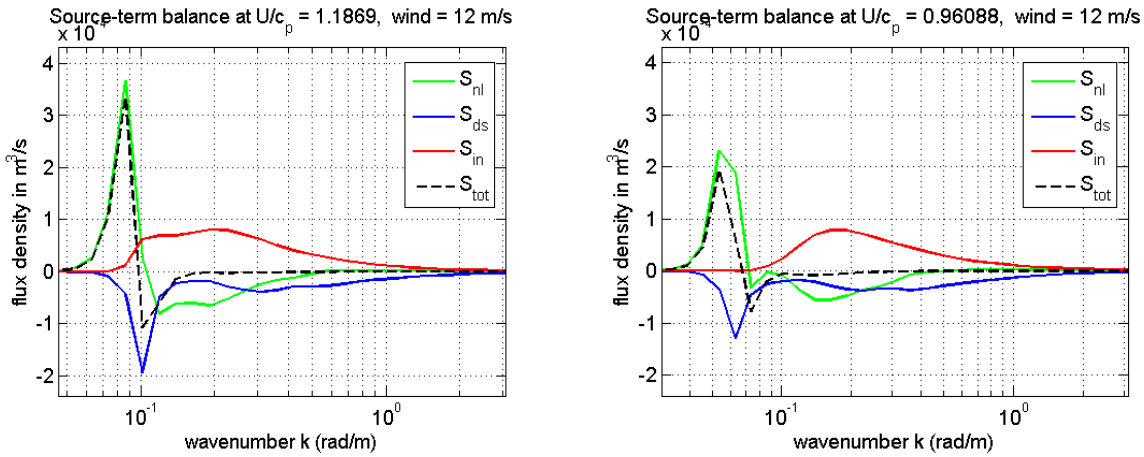

Figure 11. Source term balance for developing seas in period 1 (left panel) and maturing seas period 3 (right panel). Note the even for period 1, the spectral peak dissipation rate due to breaking is considerably larger than the wind input, as discussed in the text.

A further validation check can be made on the related matter of total wave energy dissipation rate in the water column. During the FAIRS experiment, Gemmrich and Farmer (2004) made unique measurements of the dissipation rate just below the sea surface in the presence of the breaking waves. Using the Craig and Banner (1989) model to extrapolate over the wave boundary layer and mixed layer, they estimated the total dissipation rate during period 3 was about 6.5×10^{-4} $m^3 sec^{-3}$. The corresponding level forecast for period 1 by our model is 5.5×10^{-4} $m^3 sec^{-3}$, decreasing to 4.5×10^{-3} $m^3 sec^{-3}$ for the developed seas in period 3.

We note that in order to bring the model and observations into closer agreement, the strength of the wind input source function needs to be increased marginally, particularly for the spectral peak waves. Given that the field observations of the wind input source function are limited to wind speeds generally well below 10 m/sec, it is arguably timely to revisit the issue of wind input and extend the available database to stronger wind conditions.

5. Conclusions

The availability of spectral wave breaking data gathered synchronously with the usual wind and wave height data during the recent FAIRS field investigation has allowed a significant refinement to our understanding of the evolution of wind waves. In particular it provides a strong constraint on the source terms representing the wind input and dissipation due to wave breaking.

We have investigated the performance of a spectral dissipation rate source term based on the observed breaking threshold behaviour of the normalized spectral saturation. Overall, we were able to predict breaking properties of the dominant wind seas that matched the observations for developing and mature seas. This signals a significant advance that will allow the provision of additional sea state forecast information of societal benefit.

The new breaking data for developing seas also serves to constrain the wind input source term far more closely than was possible previously. For example, we found that the

Hsaio-Shemdin (1983) form for the wind input is simply too weak in the spectral peak region to produce the observed wave energy growth and the observed dominant wave breaking levels for the developing wind seas.

Using more physically realistic forms of the wind input source term and energy dissipation rate will benefit both the reliability and utility of wave forecasts, especially with the present goal of coupling wave models to the upper ocean. This model study highlights the need to refine present observational knowledge of the wave boundary layer, in addition to the wind input source term, during higher wind and sea state conditions.

Acknowledgements

The authors gratefully acknowledge the research support for this project received from the Office of Naval Research under the CBLAST Departmental Research Initiative, and from the Australian Research Council. Special thanks also to Johannes Gemmrich for providing the breaking wave observational results, Don Resio for access to his S_{nl} code and Ekaterini Kriezi for her technical assistance during the early stage of this project.

References

Alves, J.H and M.L. Banner, 2003: Performance of a saturation-based dissipation source term for wind wave spectral modelling, *J. Phys. Oceanogr.* 33, 1274-1298.

Banner, M.L., J.R. Gemmrich and D.M. Farmer, 2002: Multiscale measurements of ocean wave breaking probability. *J. Phys. Oceanogr.* 32, 3364-3375.

Banner, M.L. and W.L. Peirson, 1998: Tangential stress beneath wind-driven air-water interfaces. *J. Fluid Mech.* 364, 115-145.

Banner, M.L. and W.L. Peirson, 2006: Wave breaking onset and strength for two-dimensional deep water waves. Submitted to *J. Fluid Mech*. (June 2006)

Donelan, M.A., 1998: Air-water exchange processes. In *Physical Processes in Oceans and Lakes* (J. Imberger, Ed), AGU Coastal and Estuarine Studies 54, 19-36.

Gemmrich, J. R. & Farmer, D.M., 2004: Near-surface turbulence in the presence of breaking waves. *J. Phys. Oceanogr*, 34, 1067-1086.

Gemmrich, J., 2005: On the occurrence of wave breaking. Proc. Hawaiin Winter Workshop on Rogue Waves, Eds. P. Muller and D. Henderson, U. Hawaii SOEST, pp 123-130

Holthuijsen, L.H., and T.H.C. Herbers, 1986: Statistics of breaking waves observed as whitecaps in the open sea. *J. Phys. Oceanogr.*, 16, 290-297.

Hsiao, S.V., and O.H. Shemdin, 1983: Measurements of wind velocity and pressure with a wave follower during MARSEN. *J. Geophys. Res*., 88, 9841-9849.

Hwang, P.A., D.W. Wang, E.J. Walsh, W.B. Krabill & R.W. Swift, 2000: Airborne measurements of the wavenumber spectra of ocean surface waves. Part II: Directional distribution. J. Phys. Oceanogr., 30, 2768-2787.

Janssen, P.A.E.M., 1991: Quasi-linear theory of wind-wave generation applied to wave forecasting. *J. Phys. Oceanogr.*, 21, 1631-1642.

Komen, G.J., L. Cavaleri, M.A. Donelan, K. Hasselmann, S. Hasselmann, and P.A.E.M. Janssen, 1994: Dynamics and Modelling of Ocean Waves, Cambridge University Press, Cambridge, 532pp.

Makin, V.K. and V.N. Kudryavtsev, 2001: Coupled sea surface-atmosphere model. 1. Wind over waves coupling. *J. Geophys. Res.* 104, 7613-7623.

Melville, W.K. and P. Matusov, 2002: Distribution of breaking waves at the ocean surface. *Nature*, 417, 58-63.

Melville, W.K., 1994: Energy dissipation by breaking waves. *J. Phys. Oceanogr*., 24, 2041-2049.

Miles, J.W., 1957: On the generation of surface waves by shear flows. *J. Fluid Mech.* 3, 185-204.
Phillips, O.M., 1985: Spectral and statistical properties of the equilibrium range in wind-generated gravity waves. *J. Fluid Mech.*, 156, 505-531.
Plant, W.J., 1982. A relation between wind stress and wave slope. *J. Geophys. Res.* 87, 1961-1967.
Snyder, R.L, F.W. Dobson, J.A. Elliott, and R.B. Long, 1981 : Array measurements of atmospheric pressure fluctuations above surface gravity waves. *J. Fluid Mech.* 102, 1-59.
Terray, E.A., M.A. Donelan, Y.C. Agrawal, W.M. Drennan, K.K. Kahma, A.J. Williams III, P.A. Hwang, and S.A. Kitaigorodskii, 1996: Estimates of kinetic energy dissipation under breaking waves. *J. Phys. Oceanogr*., 26, 792-807.
Tracy, B.A. and D.T. Resio, 1982: Theory and calculation of the nonlinear energy transfer between sea waves in deep water, WIS Rept 11, US Army Engineers Waterway Experiment Station.
Young, I.R., 1999: Wind generated ocean waves. Elsevier, 288 pp.